

6. ANALYSIS OF HISTORICAL DATA SETS

6.1 OVERVIEW

Seasonal observations of whale shark abundance recorded by ecotourism operators at Ningaloo Reef from 1995-2004 provide a historical data set that can be used to investigate temporal patterns in abundance of whale sharks in relation to oceanographic phenomenon and decadal trends in population composition and size. These records were compared with regional and global oceanographic and atmospheric variables, including average weekly sea surface temperatures (SST), along-shelf wind shear (WS), sea level (SL) and the Southern Oscillation Index (SOI). Estimates of these physical variables were derived from either ground-based data or from remote-sensing instruments. We applied generalised linear mixed-effects models (GLMM) with random sampling and model simulation to determine the relationships between the number of whale sharks and all model variants of the environmental parameters. Models were contrasted using information-theoretic weights of evidence. The SOI had the most support for explaining the deviance in weekly whale shark abundance at Ningaloo Reef during a season. The SOI positively influenced whale shark abundance such that during La Niña years, more sharks were sighted, and fewer were recorded during El Niño years. This may reflect changes in the strength of oceanographic processes such as the Leeuwin Current in response to the Southern Oscillation, which may act to transport sharks to the region and/or affect their prey by driving productivity events.

In addition to variation in response to oceanographic phenomena, analysis of ecotourism records shows that mean shark length declined linearly by nearly 2.0 m and relative abundance measured from ecotourism sightings (corrected for variation in search effort and environmental stochasticity) has fallen by approximately 40 % over the last decade. This population-level result confirms previous predictions of population decline based on projection models parameterised using mark-recapture estimates of survival. The majority of these changes are driven by reductions in the number of large individuals in the population. Phenomenological time series models support a deterministic (extrinsic) decline in large females, although there was some evidence for density dependence in large males. These reductions have occurred despite the total protection of whale sharks in Australian waters. As this species is highly migratory, the rapid change in population composition over a decade (< 1 whale shark generation) supports the hypothesis of unsustainable mortality in other parts of their range (e.g., overfishing), rather than the alternative of long-term abiotic or biotic shifts in the environment. As such, effective conservation of whale sharks will require international protection, and collaborative tagging studies to identify and monitor migratory pathways.

6.2 OCEANOGRAPHIC AND ATMOSPHERIC PHENOMENA INFLUENCE THE ABUNDANCE OF WHALE SHARKS AT NINGALOO REEF, WESTERN AUSTRALIA

6.2.1 Introduction

Whale sharks (*Rhincodon typus*), the largest fishes in the ocean (attaining sizes > 12 m in length), have a global tropical and warm-temperate distribution (Last & Stevens 1994). This wide-ranging species (Wilson et al. 2006, Bradshaw et al. 2007, Castro et al. 2007) aggregates seasonally at several coastal locations around the world (Clark & Nelson 1997, Gunn et al. 1999, Heyman et al. 2001, Meekan et al. 2006, Wilson et al. 2006, Rowat et al. 2007), making the species the target of lucrative ecotourism operations (Colman 1997, Davis et al. 1997). Whale sharks are suction filter feeders and their occurrence in coastal waters is believed to coincide with productivity events that provide an ample supply of zooplanktonic food (Taylor & Grigg 1991, Taylor 1996, Clark & Nelson 1997, Gunn et al. 1999, Heyman et al. 2001, Wilson et al. 2001a). Although various studies have attributed the aggregations of whale sharks off Ningaloo Reef to feeding as opposed to reproduction (given that a major proportion of the observed whale sharks are sexually immature males – Meekan et al. 2006), few studies have attempted to verify how the abundance of whale sharks is influenced by other environmental variables (Gunn et al. 1999, Wilson et al. 2001a).

A variety of oceanographic and atmospheric variables are known to influence the spatio-temporal abundance of pelagic and migratory marine organisms. The relative importance of these variables to a particular organism will depend on the spatial scale at which these processes operate and the functional importance of this scale to the organism. El Niño-Southern Oscillation (ENSO) is a global atmospheric process that is described by the Southern Oscillation Index (SOI) as the mean sea-level pressure difference between the central Pacific (Tahiti) and the north-eastern Indian Ocean (Darwin). In years when the sea-level pressure is higher in Pacific than the Indian ocean (a La Niña year), trade winds drive stronger currents and warmer sea temperatures along the north of Australia, positively influencing the southward flow of the Leeuwin Current along the west coast of Australia where whale sharks aggregate annually between March and June off Ningaloo Reef (Pearce & Phillips 1988, Caputi et al. 1996).

Wilson *et al.* (2001a) demonstrated that uncorrected total counts of whale sharks at Ningaloo between 1993 and 1998 were moderately correlated with the SOI, yet weakly correlated with local oceanographic variables such as sea level (SL) and sea surface temperature (SST). They concluded that inter-annual variation in the strength of the Leeuwin Current (related to the SOI rather than SL) had a greater influence on whale shark abundance than local-scale processes, presumably due to the active-transport mechanism, or directional cues provided by the Leeuwin Current. However, results of the Wilson *et al.* (2001a) study were potentially biased by inconsistent sampling strategies used

in the collection of shark abundance data and the limited temporal extent of sampling periods. Furthermore, abundance data were not corrected for variation in sampling effort among years and they did not determine how these oceanographic variables correlated with whale shark sightings at shorter temporal scales of months or weeks.

Here, we build on the work of Wilson *et al.* (2001a) by analysing a larger time series of whale shark observations from Ningaloo Reef that has been corrected for sampling effort (number of hours of observation). We also use a larger range of environmental variables and a more statistically rigorous method to determine how ocean and atmospheric processes may influence whale shark abundance. In addition to using a time series of SOI values, we use *in situ* measurements of sea level (SL) from a tide gauge and wind shear from a weather station situated close to those where whale shark sightings were recorded. We aim to estimate better the effect of physical oceanographic variables on whale shark abundance and understand this relationship in the context of the Leeuwin Current (Pearce & Phillips 1988).

6.2.2 Methods

6.2.2.1 Whale shark abundance data

We accessed an relative abundance dataset spanning from 1995 to 2004 of whale shark observations recorded from ecotourism vessels at Ningaloo Reef (Colman 1997). The area surveyed for whale sharks by ecotourism operators encompassed the northern and southern sections of the Ningaloo Marine Park in the Indian Ocean on the Northwest Cape of Western Australia (21° 40' S to 23° 30' S and 113° 45' E to 114° 15' E), which spans approximately 260 km of coastline from north to south. The number of whale sharks encountered by each operator each day during the months of April and May (the peak of the whale shark season) and the search time (effort) was recorded in a standardised log sheet as a licensing requirement for operators by the West Australian Department of Environment and Conservation (DEC) (formerly the Department of Conservation and Land Management). These data were used to calculate the average daily, weekly and monthly abundance of whale sharks and search effort.

6.2.2.2 Oceanographic and atmospheric parameters

Daily and monthly SOI values were acquired from the Australian Bureau of Meteorology and weekly values were subsequently calculated using running mean sea level pressure values (MSLP) between Tahiti and Darwin with the base period of 1932-1999. The temporal span of the SOI data was consistent with that of the whale shark abundance dataset. Sea level (SL) data were collected hourly from a tide gauge deployed at Milyering (21° 1.816' S and 113° 55.316' E) in the northern section of the Marine Park from 1998. The data were corrected to remove the effects of tides and inertial signals using a low-pass filtering technique where values were smoothed (averaged) over 30 hours. Daily, weekly and monthly average SL values were calculated. Sea surface temperature (SST) is known to predict biologically important changes in fish

abundance (Iwasaki 1970, Fiedler & Bernard 1987). SST data were calculated from daily and weekly composites of 4-km resolution NOAA Advanced Very High Resolution Radiometer (AVHRR) satellite images of the Ningaloo region (21° S to 24° S and 112° E to 115° E). The 4 × 4 km pixel values in the composites were spatially averaged to obtain single daily and weekly SST values.

Wind shear (WS) was hypothesised to correlate with whale shark abundance because it is a good proxy for the strength and direction of wind along the shelf, and thus related indirectly to the strength of the Ningaloo Current, an inshore counter current that is believed to be important for retaining planktonic biomass along Ningaloo Reef (Taylor & Pearce 1999). Wind speed and direction data were collected half-hourly at a weather station at Milyering from 1997. These were used to calculate an along-shelf wind vector or wind shear parameter that was a length vector calculated by combining wind direction and speed and rotating the data clockwise at 60° (relative to true north). Currents and winds were also rotated to along- and cross-shelf components. The same low-pass filtering technique used for SL was also used for wind shear and the resulting values averaged on daily, weekly and monthly intervals.

We also explored the utilisation of weekly maps from a variety of remotely sensed and point-source data for determining the influences of other biophysical properties on whale shark abundance. We generated maps of weekly surface geostrophic currents (surface current estimates that relate directly to sea surface topography and the Coriolis force) using Topex/Poseidon altimetry data (www.aviso.oceanobs.com) with a spatial resolution of 0.1 degrees (latitude/longitude). Maps were made in ArcGIS 9.1 according to calculations described by (Polovina et al. 1999), where U and V vectors were calculated and then decomposed into compass direction (degrees True North) and velocity (cm/s-1). Weekly chlorophyll-*a* maps with 9-km spatial resolution were derived from Sea-viewing Wide Field-of-view Sensor (SeaWiFS) level 3 (version 5.1) Global Area Coverages (GAC) using SeaDAS 4.8 ocean color software (developed by the US National Aeronautics and Space Administration – NASA). While some of these additional data helped to illustrate general patterns in oceanographics, we refrained from including weekly maps of chlorophyll-*a* concentration (e.g., SeaWiFS) and geostrophic currents/mean sea surface height (e.g., Topex/Poseidon altimetry) in any further analysis since large areas without data were frequently present in maps due to atmospheric interference or due to coastal/land mask generalisation.

6.2.2.3 Analysis

A series of generalised linear mixed-effects models (GLMM) were used to explore relationships between oceanographic and atmospheric variables and relative whale shark abundance at Ningaloo Reef. Examination of the residuals for the saturated models determined the statistical family (i.e., Gaussian, gamma etc.) and error distribution most appropriate for each analysis. In this case, a gamma error distribution with a log link function was most appropriate. The error structure of GLMM corrects for non-independence of statistical units (relative abundance estimates) due to shared temporal structure (months), and permits the 'random effects' variance explained at different levels of

clustering (months) to be decomposed. All oceanographic and atmospheric variables were modelled as fixed effects.

Model comparison was based on Akaike's Information Criteria corrected for small samples (AIC_c), (Burnham & Anderson 2002). Model AIC_c were ranked, with the most parsimonious model(s) having the lowest AIC_c values and highest model weights (Lebreton et al. 1992). From the set of *a priori* models we used a predictive model averaging procedure to determine the magnitude of the effect of some terms, keeping all other dependent variables constant (Burnham & Anderson 2002). The weights of evidence (w_{+i}) for each variable were calculated by summing the model AIC_c weights (w_i) over all models in which each term appeared. However, the w_{+i} values are relative, not absolute because they will be > 0 even if the predictor has no contextual explanatory importance (Burnham & Anderson 2002). To determine the predictors that were relevant to the data, a baseline for comparing relative w_{+i} across predictors was required. Following Burnham & Anderson (2002), we randomised the data for each predictor separately within the dataset, re-calculated w_{+i} , and repeated this procedure 100 times for each predictor. The median of this new randomized w_{+i} distribution for each predictor was taken as the baseline (null) value (w_{+0}). For each term the relative weight of evidence (Δw_{+}) was obtained by subtracting w_{+0} from w_{+i} . Predictors with Δw_{+} of zero or less have essentially no explanatory power. All statistical analyses were done using the R Package (R Core Development Team 2004).

We separated the modelling component into a hierarchy based on the extent of the time series for each environmental variable. Only SOI and SST data available for the full dataset of whale shark abundance (1995–2004), so these and all combinations of these variables were used for the initial model (all-subsets). Sea level and wind shear were only available from 1998-2004. Consequently, the second model used four environmental variables (SOI, SST, SL and WS) and all combinations of these to determine how they influenced weekly whale shark abundance from 1998 to 2004. A Spearman's correlation analysis was done for each set of variables in each model. Highly correlated ($r > 0.8$) variables were not included in the same model. The percentage of deviance explained (D) was also calculated for each model as a measure of goodness-of-fit.

6.2.3 Results

6.2.3.1 Relative abundance of whale sharks 1995-2004

Within the annual period (March to July) when whale sharks attend the area off Ningaloo Reef, the highest abundances were observed in early April 1995 and 1996, and towards the end of May in 2002 (Fig. 6.1a & b). In most years, weekly whale shark sightings were clustered between the beginning of April and the beginning of June, with few sighting occurring at the start of March or at the end of June.

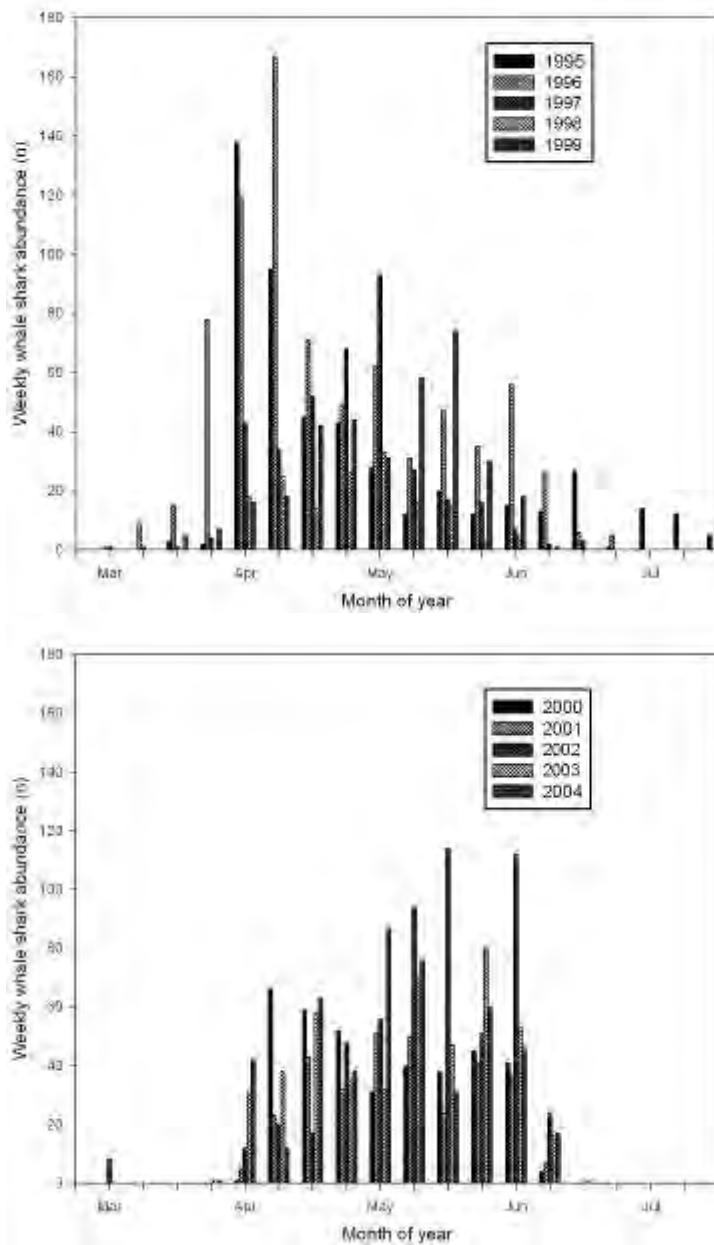


Figure 6.1. The weekly abundance of whale sharks observed off Ningaloo Reef from March to July between years (a) 1995 – 1999, and (b) 2000 – 2004.

6.2.3.2 Weekly SOI and SST from 1995-2004

SOI and SST were weakly correlated (0.28, Table 6.1). The model that included the Southern Oscillation index (SOI) was the best in the set of possible models for explaining the variation in weekly abundance of whale sharks between 1995 and 2004 (8.9 % deviance explained, Table 6.2). The weights of evidence revealed that the SOI term had the highest contribution to model fits ($\Delta w_i = 0.30$). In general, there was a positive relationship between weekly whale shark abundance at Ningaloo Reef and SOI values in 1995-2004 suggesting that more whale sharks were observed in weeks with a characteristic La Niña signal while relatively few sharks were observed in weeks with a strong El Niño signal (Fig. 6.2).

Table 6.1: Correlation matrix between Southern Oscillation index (SOI), sea surface temperature (SST), sea level (SL) and along shelf wind shear (WS) from 1998-2004.

	SOI	SST	SL
SST	0.292	-	-
SL	0.512	0.419	-
WS	0.091	0.074	0.502

Table 6.2: Generalised linear mixed-effects models and information-theoretic statistics based on the change in Akaike's Information Criterion corrected for small samples (ΔAIC_c) for model scenario 1 using Southern Oscillation index (SOI) and sea surface temperature (SST) to estimate trends in weekly whale shark abundance from 1995-2004. Notations; D = % deviance explained ΔAIC_c = change in AIC_c between models, w_i = AIC_c weight.

Model	D	ΔAIC_c	w_i
SOI	8.904	0.000	0.424
SST	3.270	1.949	0.159

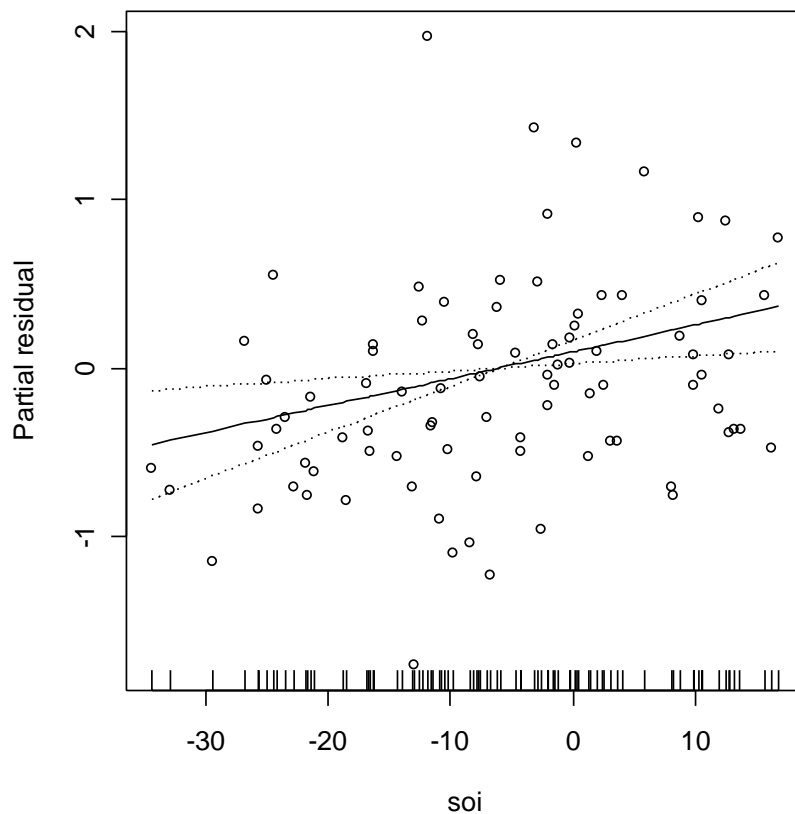


Figure 6.2. Partial residual plot generated from the most-parsimonious generalized linear model relating weekly whale shark abundance between 1995 and 2004 to the Southern Oscillation index (SOI). The solid line is the fitted linear model. The dashed lines are the approximate 95 % point-wise confidence intervals.

6.2.3.3 Weekly SOI, SST SL and WS from 1998-2004

Of all the variables, only SOI and sea level were moderately correlated (0.512, Table 6.1). Despite several competing models (Table 6.3) only SOI and SST had sufficient evidence for explaining variance in whale shark abundance ($\Delta w+ = 0.19$ and 0.15 , respectively). Both these variables were positively correlated with whale shark abundance (Fig. 6.3), yet the model that included only SOI was able to explain a larger amount of the deviance in the data compared to a model that included SST or a model that included both SST and SOI. This suggested that SOI had the best predictive capacity for explaining the weekly abundance of whale sharks at Ningaloo Reef.

Table 6.3: Generalised linear mixed-effects models and their information-theoretic statistics based on the change in Akaike's Information Criterion corrected for small samples (ΔAIC_c) for model scenario 2 using Southern Oscillation index (SOI), sea surface temperature (SST), sea level (SL) and wind shear (WS) to estimate trends in weekly whale shark abundance from 1998-2004. Notations; D = % deviance explained, ΔAIC_c = change in AIC_c between models, w_i = AIC_c weight.

Model (i)	D	ΔAIC_c	w_i
SOI + WS	26.152	0.000	0.218
SST + WS	24.585	0.343	0.183
WS	14.804	0.548	0.165
SOI + SST+WS	30.894	0.962	0.134
SL + WS	19.408	1.476	0.104

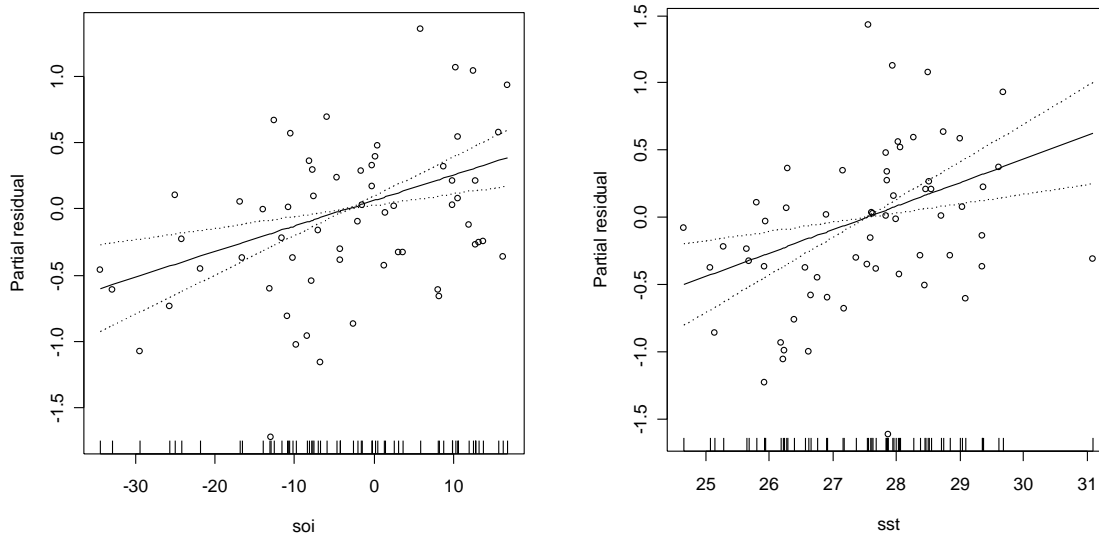


Figure 6.3. Partial residual plots generated from the most-parsimonious generalized linear model relating weekly whale shark abundance between 1998 and 2004 to the Southern Oscillation index (SOI) and sea surface temperature (SST). The solid lines represent the fitted linear models. The dashed lines are the approximate 95 % point-wise confidence intervals.

6.2.4 Discussion

Of the atmospheric and oceanographic variables that were hypothesised to influence whale shark abundance at Ningaloo Reef, only the SOI appeared to be related to shark numbers. In the analysis of the longest time series of environmental and abundance data (1995-2004), the SOI was negatively correlated with weekly whale shark abundance. The importance of the SOI did not change even when additional environmental variables were included in the models, and the weekly dataset of shark abundance was truncated (1998-2004). There was some support for SST having an influence on relative whale shark abundance, although unlike the SOI, there is likely to be high spatial variation in SST at scales of 1 to 100 km Sumner et al. 2003. Weekly AVHRR satellite image composites captured during times when whale shark abundances are peaking at Ningaloo, illustrate the presence of high SST's in the north – eastern Indian Ocean extending south past Ningaloo reef where mixing with cooler surface water occurs (Figure 6.4). A clearer analysis of the relationship between SST and whale shark abundance requires a more explicit spatial and temporal assessment which is likely to come through future tagging studies. Surprisingly, sea level had little influence on whale shark abundance, despite its strong correlation with the strength of the Leeuwin Current and SOI (Pearce & Phillips 1988).

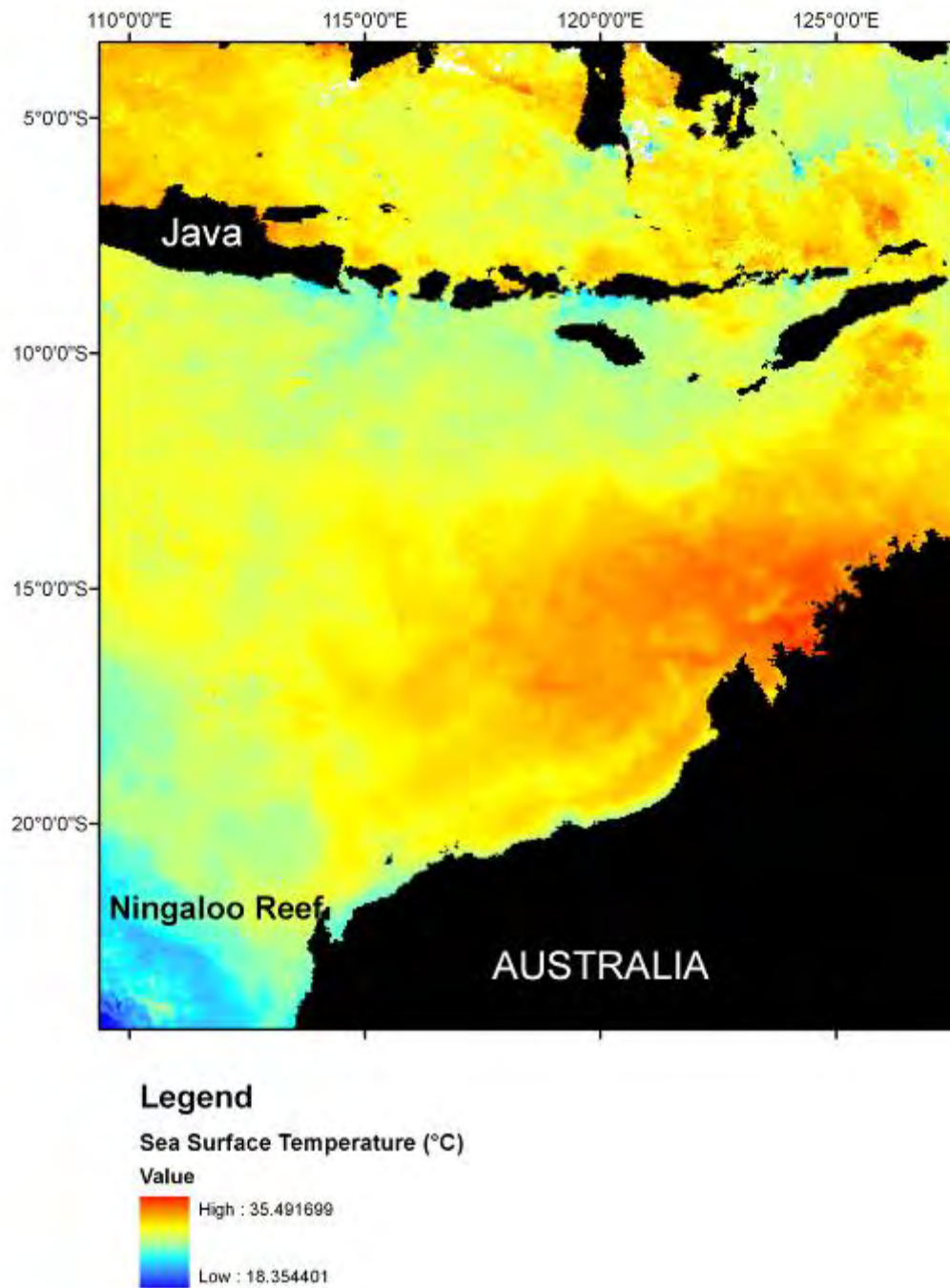


Figure 6.4. Weekly AVHRR satellite image composite of sea-surface temperature variability in the East Indian Ocean during the annual period when average whale shark abundances tend to be high (1st week of May).

Our results based on corrected data and using a rigorous multi-model inferential approach (Burnham & Anderson 2002) supported the findings of Wilson *et al.* (2001a) who also suggested that SOI was an important factor influencing the abundance of whale sharks at Ningaloo Reef. The SOI is effectively a measure of ENSO, a large-scale climatic process that has two climatic phases: El Niño and La Niña. During the latter, strong Pacific trade winds and warmer sea temperatures (also known as the Walker circulation) in the ocean north of Australia act to increase the strength of a variety of ocean currents, notably the Indonesian Through-Flow and the East Gyral current and ultimately the southerly flowing Leeuwin Current (Rochford 1962, 1984) (Fig. 6.5a & b). These currents may influence the abundance of whale sharks at Ningaloo Reef in two ways; first, by providing a transport mechanism (i.e., currents - geostrophic flow) for sharks to the Ningaloo region and second, by acting as the drivers of coastal upwelling and productivity events (increased chlorophyll- α) that increase zooplankton abundance for filter-feeding sharks. While we cannot retrospectively determine the configuration of currents in the north eastern Indian Ocean during the times when high abundances of whale sharks were observed at Ningaloo, we can make some inferences about surface current structure through the use of Altimetry data. Geostrophic surface flow vectors (generated from Topex/ Poseidon Altimetry -Sea Surface height data) show cyclonic and anti-cyclonic circulation (eddies) present offshore during periods of high whale shark abundance (Fig. 6.6). These might influence numbers by entraining sharks and transporting them southwards toward the reef.

Ocean colour satellite imagery (SeaWiFs) indicates the presence of high chlorophyll- α concentrations in the surface waters in the Gulf of Exmouth (adjacent to Ningaloo) and in anomalous 'highly mixed' water bodies off the shelf from Ningaloo reef during the period when whale sharks are in peak abundance (Fig. 6.7). These relationships are intriguing, but require further investigation to determine how primary production equates spatially with secondary production and the subsequent availability of food to whale sharks.

A long-term (decadal) photo-identification study of whale sharks at Ningaloo Reef has shown that many sharks are resighted in successive years at this locality (Meekan *et al.* 2006, Bradshaw *et al.* 2007). Tagging studies using Pop-up archival tags (PSAT) show that following aggregations, whale sharks move northward from Ningaloo (Wilson *et al.* 2006). Tags that detach from whale sharks < 4 to 5 months after deployment are typically found on the continental shelf to the north, while tags that detach after this time have been found in the open ocean beyond the continental shelf. Wilson *et al.* 2006 suggested that this indicates that whale sharks could be using the directional cues of the northward-flowing current systems such as the Ningaloo Current to migrate northwards along the shelf after visiting Ningaloo and then later move offshore to take advantage of the southward-flowing Leeuwin Current to return to the reef. A weakening or strengthening of the Leeuwin Current as a result of the ENSO phenomenon might thus account for the correlation between the SOI and relative whale shark abundance.

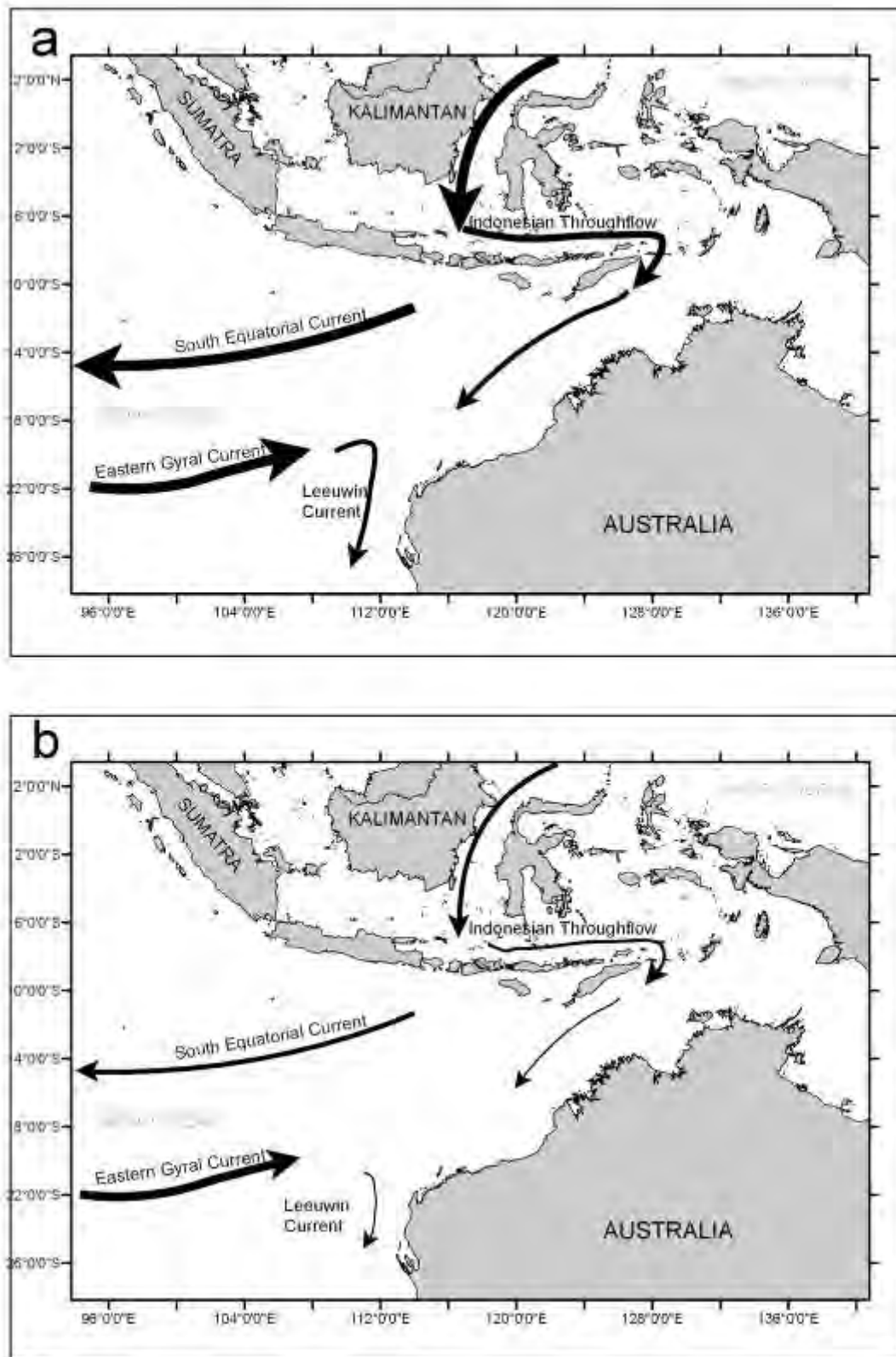


Figure 6.5. Oceanographic models indicating the relative differences in the circulation patterns and strength of major currents (as denoted by thickness of arrows) in the North East Indian Ocean during (a) La Niña and (b) El Niño climatic periods.

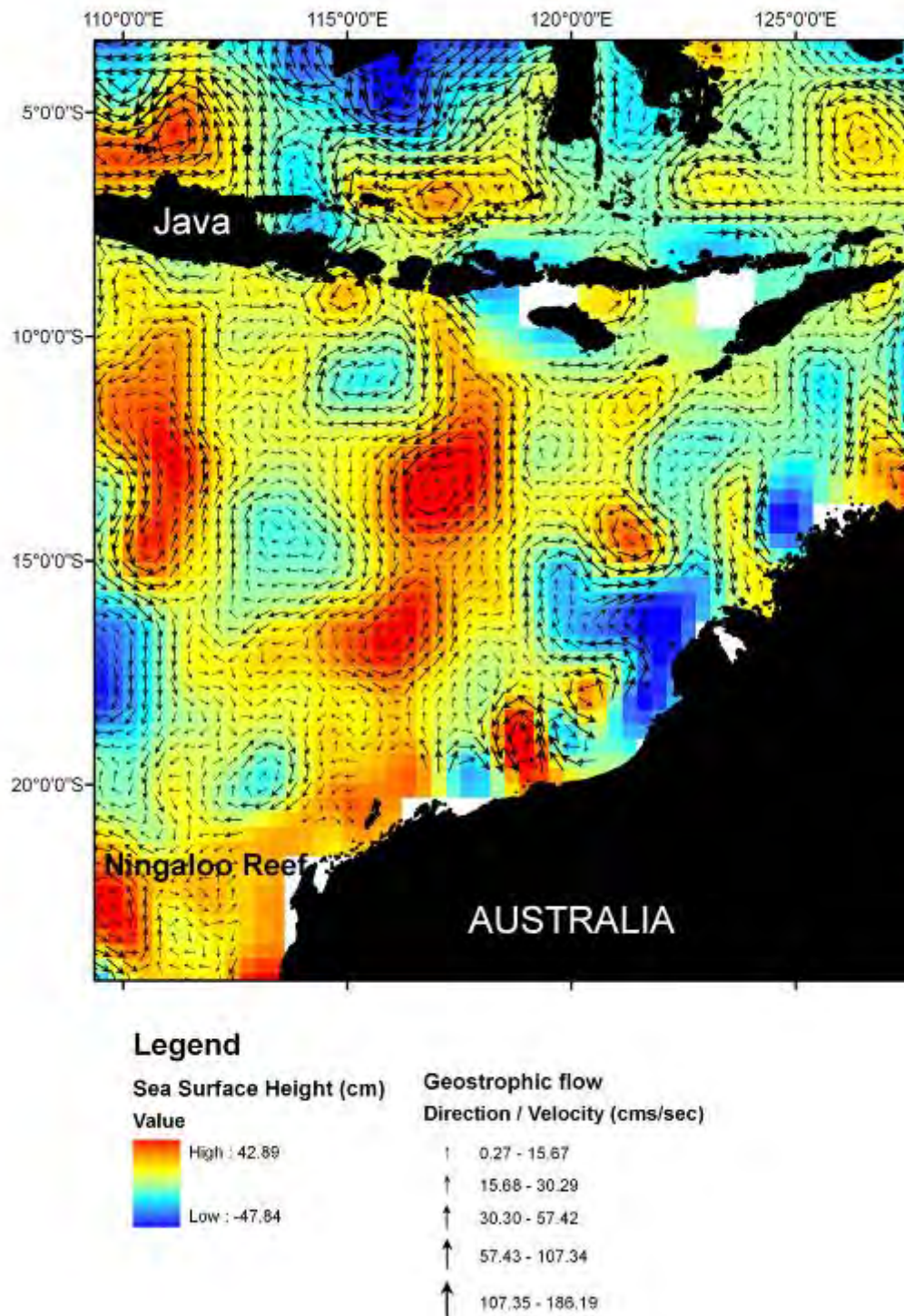


Figure 6.6. Weekly Topex/ Poseidon altimetry composite of Sea Surface height and associated geostrophic flow (direction and velocity) in the East Indian Ocean during the annual period when whale shark abundances tend to peak (1st week of May).

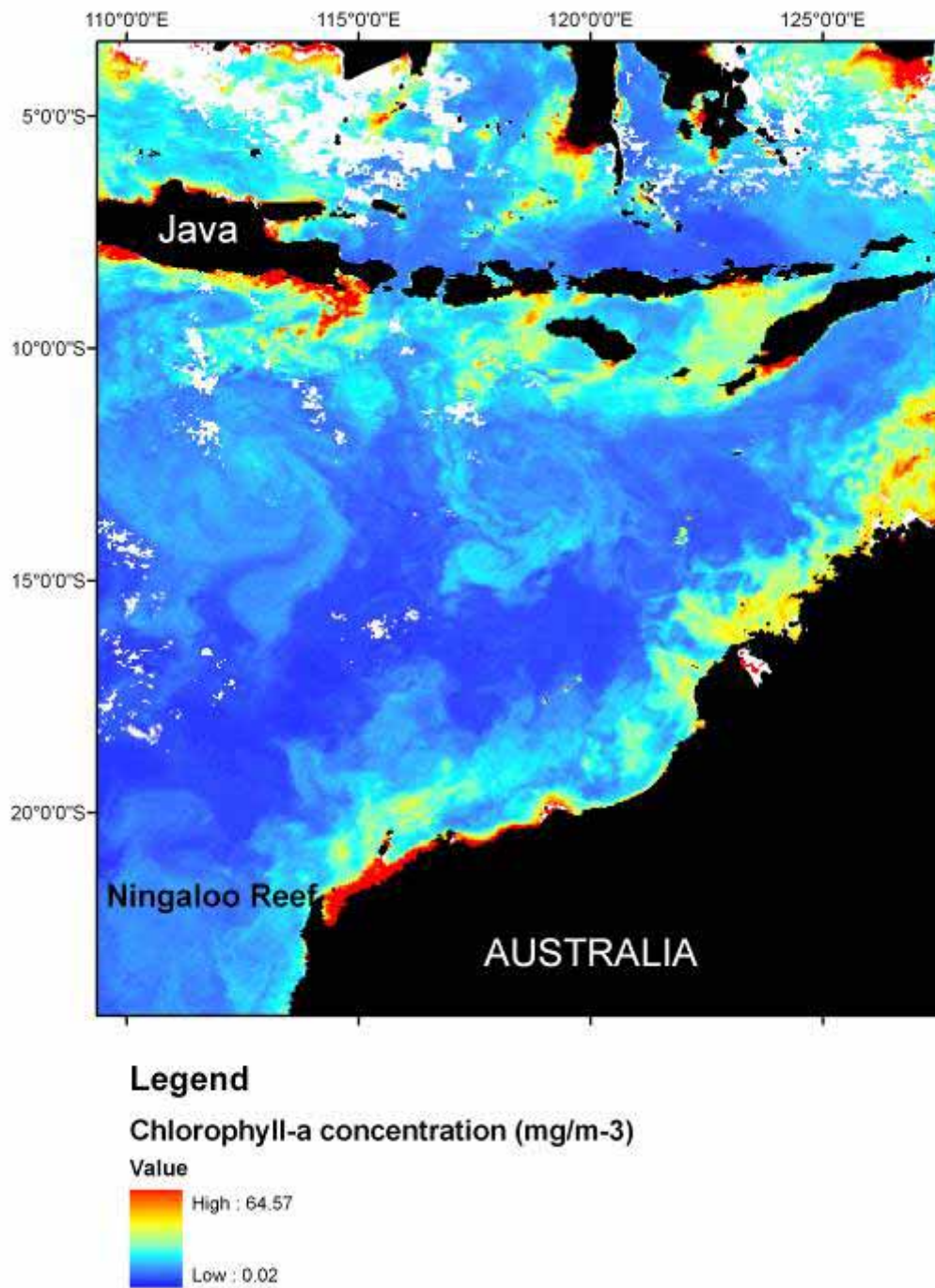


Figure 6.7. Weekly SeaWiFs satellite image composite of chlorophyll-a concentration in the East Indian Ocean during the annual period when whale shark abundances tend to peak (1st week of May).

The influence of the ENSO climatic signal is not limited to physical effects on currents. Variation in the strength, timing and path of the Leeuwin Current due to ENSO has cascading effects on the types and abundances of marine organisms that occur on the Western Australian coastline (Caputi et al. 1996). For instance, recruitment of the western rock lobster (*Panulirus cygnus*) is positively influenced, while recruitment of scallops (*Amusium balloti*) and pilchards (*Sardinops sagax neopilchardus*) are negatively influenced. These annual differences probably reflect changes in the food chains and the availability of the appropriate prey for larval or young stages. For whale sharks, it is possible that La Niña climatic episodes influence abundance on Ningaloo Reef by favouring the oceanographic conditions necessary for the proliferation of their prey. While the strong Pacific trade winds characteristic of La Niña are important for driving the warm, southerly-flowing Leeuwin Current, the strength of this current also positively influences the flow of the cooler Ningaloo counter-current. The Ningaloo Current predominates on the reef front from September to April, and is believed to influence coastal upwelling with prevailing South Westerly winds due to Ekman transport (Holloway & Nye 1985, Taylor & Pearce 1999, Holloway 2001). This upwelling determines localised productivity events along the Ningaloo coast, which may attract whale sharks to the reef (Taylor & Pearce 1999). In temperate regions there is some evidence that large-scale climatic phenomena influence the abundance of planktivorous sharks (e.g., basking sharks *Cetorhinus maximus*) by driving oceanographic events that alter productivity of coastal waters and ultimately the availability of zooplankton food (Squire 1990, Sims & Quayle 1998).

It is still a challenge to determine how changes in the strength of current systems in response to the ENSO phenomenon may act to transport sharks to the region and/or indirectly affect their prey by driving productivity events at Ningaloo Reef. This issue is currently under investigation through the deployment of satellite tags so that whale shark migrations can be linked to oceanographic processes observed from remotely sensed data. Satellite measurements of chlorophyll *a* concentrations and other potentially important parameters (e.g., SST and salinity) can be overlaid on migration pathways to determine the extent to which whale shark aggregations are related to physical transport mechanisms and productivity of Ningaloo Reef.

6.3 DECLINE IN WHALE SHARK SIZE AND ABUNDANCE AT NINGALOO REEF OVER THE PAST DECADE: THE WORLD'S LARGEST FISH IS GETTING SMALLER

6.3.1 Introduction

The effects of overfishing reach far beyond the relatively predictable reduction of yields (Food and Agriculture Organisation of the United Nations 2006); overfishing of marine species can also disrupt important biological processes by removing particular size classes (Walker 1998), thereby changing an exploited population's age structure, individual maturation times and growth rates (Myers et al. 1995, Jennings & Kaiser 1998, Jennings et al. 1998, Dulvy et al. 2003, Reynolds et al. 2005). Changes to demographic rates and the evolutionary patterns induced by size-selective fishing can increase extinction risk in harvested species (Jennings & Kaiser 1998, Jennings et al. 1998, Conover & Munch 2002, Reynolds et al. 2005), so measuring changes in size structure is an important step in identifying whether over-exploitation has occurred (Shin et al. 2005, Greenstreet & Rogers 2006).

Many large pelagic species such as tunas, billfishes and sharks that are targeted directly or are taken as bycatch in industrial fisheries have experienced substantial declines over the last century (Baum et al. 2003, Sibert et al. 2006, Myers et al. 2007). For sharks in particular, high harvest rates mainly from bycatch have resulted in rapid population declines (Baum et al. 2003, Robbins et al. 2006, Sibert et al. 2006, Myers et al. 2007), although the dynamics of the interacting drivers of decline make predictions of extinction risk difficult (Walker 1998, Stevens et al. 2000, Baum et al. 2003, Baum et al. 2005, Burgess et al. 2005a, b, Robbins et al. 2006). Additionally, these population crashes have occurred in spite of the perceived lower extinction risk of broad-ranging and wide-dispersing species (Terborgh & Winter 1980).

Although harvested to an unquantified extent (Chen et al. 1997a, Chen & Phipps 2002), the world's largest fish, the whale shark (*Rhincodon typus* Smith, 1828), also appears to have declined throughout much of its range (CITES 2002, Theberge & Dearden 2006, Bradshaw et al. 2007). These wide-ranging (Eckert et al. 2002, Wilson et al. 2006, Bradshaw et al. 2007, Castro et al. 2007) filter feeders are distributed throughout the world's tropical and warm temperate seas and are classed as *Vulnerable* under IUCN Red List criteria and listed by the *Convention on International Trade in Endangered Species of Wild Fauna and Flora* (CITES) in *Appendix II* (i.e., "species not necessarily threatened with extinction, but in which trade must be controlled in order to avoid utilization incompatible with their survival") (CITES 2002). Like most shark species, whale shark have slow growth rates, late maturity and extended longevity (Frisk et al. 2001, Bradshaw et al. 2007, Graham & Roberts 2007), and such traits are likely to limit annual recruitment and increase susceptibility to over-exploitation by humans (Smith et al. 1998, Bradshaw et al. 2007). The high degree of connectivity among aggregations at broad spatial scales (Castro et al. 2007,

Graham & Roberts 2007) suggests that unsustainable fishing mortality at one locality will affect unexploited aggregations at another (Bradshaw et al. 2007).

In the late 1980s, aggregations of whale sharks were reported in coastal waters at a few locations in Australia, Southeast Asia and the Caribbean (Taylor 1996, Heyman et al. 2001). Since this time, the predictability of seasonal aggregations has fostered the development of a profitable ecotourism industry (Meekan et al. 2006, Graham & Roberts 2007). Ecotourism at Ningaloo Reef, Western Australia, one of the world's largest whale shark aggregations, began in the early 1990s and since 1995, location, sex and length data have been recorded for most individuals encountered (Meekan et al. 2006). This industry uses light aircraft to locate the sharks in surface waters and to direct vessels into their path so that paying tourists are able to swim with the slow-moving sharks (Davis et al. 1997). Whale sharks come to Ningaloo Reef from March to June, where they are found in shallow water (< 100 m) along the front of the fringing coral reef (Taylor 1996). These continuous records now span a decade, providing a large sightings dataset that offers insight into this aggregation's demography and population status.

Based on the anecdotal and catch evidence that the whale shark population has experienced (largely unmeasured) exploitation in the Indian Ocean basin (Chen et al. 1997a, Chen & Phipps 2002), we hypothesised that evidence for over-exploitation would be revealed by an observed decline in larger (older) individuals (Stergiou 2002). Previous work using photo-identification of 159 known individuals at Ningaloo Reef has provided some support for this hypothesis, with an observed increase in the proportion of small (< 6.7 m total length) sharks (Meekan et al. 2006). Here we used a much larger and independently collected dataset to test for a continuous reduction in average shark size (total length). There are three main mechanisms that may drive changes in body size of harvested populations: (1) abiotic factors affecting growth and development (e.g., large-scale climate or regime shifts); (2) biotic changes such as density-modified growth rates and (3) changes to demography and genetic composition via harvesting (Ratner & Lande. 2001). We therefore explicitly examined the form of the decline (linear, logistic or quadratic) to test for the presence of a new mean size equilibrium. We hypothesised that a rapid, deterministic mortality source of a particular size class (e.g., size-biased harvest) might induce a gradual decline in mean size followed by a tapering toward a new equilibrium size as larger individuals were systematically removed from the population. By comparison, sustained linear decline without tapering may indicate a shift by fishers to target progressively smaller individuals as larger individuals are depleted from the population (cf. Pauly et al. 1998).

A natural corollary of over-exploitation is the prediction that overall abundance of the population decreases (Food and Agriculture Organisation of the United Nations 2006); as such, we tested the hypothesis that the number of whale sharks seen at Ningaloo Reef has changed since monitoring began. This hypothesis is based on previous capture-mark-recapture model estimates of survival and matrix projections that inferred long-term decline of whale sharks visiting Ningaloo Reef (Bradshaw et al. 2007). Using the large operator-

collected dataset, we tested the hypothesis of a decline directly using relative abundance data corrected for sampling effort and environmental stochasticity because whale shark abundance is known to fluctuate annually relative to local oceanographic conditions (Wilson et al. 2001a).

Our final aim was to gain insight into the relative contribution of demographic and environmental processes driving the population trends. We hypothesised that abundance time series from a declining population will demonstrate more support for an exponential model describing the relationship between the rate of change and population density compared to a stable population fluctuating around carrying capacity (see Brook & Bradshaw 2006). As such, we predicted that the exploited whale shark abundance time series will show little support for density regulation, and we test this explicitly by contrasting phenomenological density-dependent and density-independent models applied to the relative abundance time series. Although we focus on a single iconic species, our intent is to provide marine conservation biologists with a general approach for examining potential causes of decline in long-lived marine predators when detailed demographic data are rare and relative abundance time-series data are readily available.

6.3.2 Materials and methods

6.3.2.1 Tourist operator-collected data

Numbers of whale sharks at Ningaloo Reef peak in the months of April and May (Davis et al. 1997, Wilson et al. 2001a). Because sighting effort occurs sporadically outside of the peak months, our analysis was restricted to the peak period. Tour operators collected information on estimated total length (TL, visual estimation from the spotter plane and vessel; corroborated by in-water measurements) (Meekan et al. 2006) and sex (via the identification of claspers on males) (Taylor 1994a) for each shark observed. Licenses for tourist boat access to sharks are restricted by the Western Australian Department of Environment and Conservation (WA-DEC). This means that the same vessels tend to operate from year to year (Davis et al. 1997). There is however, turnover in crew, which should negate the possibility that any observed trends in size distribution are merely the result of year-by-year improvement in an operator's assessment skill and capacity. Supporting this, the same observed trends were consistent in data collected by licensees operating only from Coral Bay or Tantabiddi > 100 km away (B. M. Fitzpatrick, unpubl. data). Recently, WA-DEC implemented a training course that all employees of the whale shark tourism operations are required to attend, and records indicate that no single boat skipper, dive master or crew member has remained during the entire sample interval. In fact, most employees remain for an average of two years only. Additionally, spotting-plane pilots typically provide the first estimate of whale shark size, and pilots turnover at a similar rate to boat crews (B. M. Fitzpatrick, unpubl. data).

Spotter planes are generally shared between two or more tourist vessels with patrons sharing the same shark. Length estimates of the same shark are a combined effort between a plane pilot, one or more boat skippers, and in-

water shark spotters, all with varying experience. Such repeat observations of the same shark were identified in different ship logs and removed from the dataset. Length estimates of surfaced sharks are typically made by pilots and corroborated by comparison to known-length vessels in the water; further validation is provided by in-water measurements compared to known-length snorkelers. Length measurements are only entered into the database once pilots and multiple operators agree. As quantified corroboration, direct in-water measurements of sharks compared favourably to pilot and vessel-operator estimates of total length (Norman 1999).

There is little evidence that the presence of snorkelers influences whale shark behaviour. The interaction of tourists and vessels with sharks is tightly controlled by a code of conduct enforced by DEC (Davis et al. 1997). This ensures that patrons do not approach within 3 m of the shark while snorkelling, and vessels must remain a minimum of 30 m from the shark for a maximum of 90 minutes (Davis et al. 1997). Studies of whale sharks at Ningaloo Reef could find no detectable changes in behaviour of sharks in the presence of snorkelers (Norman 1999) that might bias our results.

6.3.2.2 Reduction in total length over time

To test the hypothesis of a continuous decline in mean shark size and to examine the form of this trend, four linear and nonlinear models of mean annual TL (over all individuals for which a TL estimate was made) against year were contrasted. Models represented four hypotheses: (1) no temporal trend (intercept: $TL \sim 1$), (2) linear decline (linear: $TL \sim year$), (3) curvilinear decline (quadratic: $TL \sim year + year^2$), and (4) sigmoidal decline (logistic: $TL \sim a/b \cdot e^{-year}$, where a and b are constants). Non-linear models were used in addition to linear models because distinct processes affecting mean size in a population may introduce different trends in size over time (see Introduction).

We used Akaike's Information Criterion corrected for small sample size (AIC_c) as an index of Kullback-Leibler (K-L) information loss to assign relative strengths of evidence to the different competing models (Burnham & Anderson 2002). One could also employ other methods to compare models such as the dimension-consistent Bayesian Information Criterion (BIC); however, BIC may only be preferable when sample sizes are approximately ≥ 20 data per parameter estimate (Burnham & Anderson 2002, Link & Barker 2006). The relative likelihoods of candidate models were calculated using AIC_c (Burnham & Anderson 2002), with the weight ($wAIC_c$) of any particular model varying from 0 (no support) to 1 (complete support) relative to the entire model set. For each model considered, we also calculated the percentage deviance explained (%DE) as a measure of goodness-of-fit. Information-theoretic evidence ratios (ER , an index of the likelihood of one model over another, calculated as the $wAIC_c$ of one model \div $wAIC_c$ of another model) (Burnham & Anderson 2002) were used to contrast specific model pairs.

The above analysis only examines the trend in mean total length over time. To incorporate uncertainty due to year, month and vessel into the test for a

decline in mean total length, we also applied a series of five *a priori* general linear models (GLM) with Gaussian error distributions and identity link functions, where individual TL was set as the response and the terms *year/month* were treated as a nested term and individual factors made up the various model combinations. The term *month* was included in some models to account for possible phenology changes (e.g., temporal changes arrival patterns during the peak season) that may vary with strength of the El Niño-Southern Oscillation events each year (Wilson et al. 2001a, and see below). We also considered a second set of models replacing *month* with *day of year* as a covariate to investigate whether more variance in *total length* could be explained. Models were contrasted using the Bayesian Information Criterion (BIC) given the large sample size ($n = 1814$) and our desire to distinguish main from tapering effects (Burnham & Anderson 2002, Link & Barker 2006). We also considered a second set of 8 models that included the sex effect (with a reduced overall sample size given that not all individuals could be sexed reliably; $n = 1333$). To test further the hypothesis that systematic changes in observers may have biased observed size trends, we constructed a series of linear mixed-effects models (GLMM) using the `lmer` command in the `lme4` library of the R Package (R Core Development Team 2004), coding *year* as a fixed covariate and *vessel* as a random factor.

6.3.2.3 Relative shark abundance and climate variation

Relative shark abundance was calculated by summing the total number of sharks seen for the months of April and May and dividing these values by the total search time for all observing vessels for these two months over each year of the study (SPUE = sightings per unit effort). The monthly interval was chosen to match available environmental data for sightability bias correction (see below). Search time was calculated only over the peak interval and not the entire year. The database was corrected so that a shark was only recorded once per day even though it may have been sighted by several tourist operators during that day. The majority of this 'effort' (> 90 %) is devoted to searching for sharks rather than transiting to one once it has been identified by another vessel. There is therefore little chance that extra time spent transiting between a single shark visited by several vessels would impart any important bias to indices of search effort. However, it was still possible that the same shark was seen on subsequent days (i.e., individual sharks were not marked). Tagged whale sharks remain near the Ningaloo coast for several weeks after tagging (Wilson et al. 2006), so repeated sampling of some sharks was probable. However, this problem is unlikely to affect overall size and abundance trends unless there was some systematic change in residence times that we could not record. Furthermore, given that individual sharks are unlikely to remain at Ningaloo Reef for more than a few weeks (at most), monthly comparisons of relative abundance should account for gross changes in abundance more appropriately than examining the trends at finer temporal scales.

Climate variation is thought to affect whale shark relative abundance at Ningaloo Reef (Wilson et al. 2001a). Critically, however, the relationship between whale shark abundance and El Niño-Southern Oscillation (ENSO) variation established by Wilson et al. (2001a) did not correct relative

abundance estimates for variation in search effort. The oceanography around Ningaloo Reef is dominated by the Leeuwin Current (LC), which forms from the Indonesian Through-Flow system to the north (Morrow & Birol 1998). The LC flows south along the shelf break bringing warm, nutrient-poor water to the coast of Western Australia (Pearce & Griffiths 1991). Between the LC and the coast, cooler water upwells from depth to form the Ningaloo Current, which flows along the edge of Ningaloo Reef towards the north (Morrow & Birol 1998). The relative strengths of these current systems are strongly influenced by El Niño-Southern Oscillation (ENSO) events (Pearce & Phillips 1988). During El Niño years, the LC is weak and water temperatures along the coast of Western Australia are relatively cool, while in La Niña years the current is stronger and water temperatures are higher. This variability in current flow is known to influence recruitment to many commercial fisheries in Western Australia (Lenanton et al. 1991, Caputi et al. 1996).

To correct the relative abundance data (sightings per unit effort – SPUE) for this annual climate variation, we used maximum likelihood estimation (MLE) to fit a linear regression between mean SPUE to the mean April and May Southern Oscillation Index (SOI) (calculated from a two-month running mean smoother). We then detrended the SPUE time series based on this relationship (subtracting fitted values from observed SPUE). Temporal comparisons of detrended SPUE assume, of course, that SPUE reflects relative changes in total abundance.

Photo-identification data of 159 known individuals suggest that that whale sharks at Ningaloo Reef have changed in age/size composition since monitoring began (Meekan et al. 2006). To expand on this preliminary work and to test the hypothesis with the much larger tourist operator dataset, we examined the SOI-detrended SPUE trends for four size-sex classes based on the median TL (6 m) observed over all sharks: small (< 6 m) or large (\geq 6 m), and male or female (median TL was not calculated for each sex separately due to the weak sex effect; see Results). We deliberately avoided using a putative size at maturity as the threshold for dividing ‘small’ and ‘large’ sharks, given the uncertainty associated with this value (Bradshaw et al. 2007). Our aim here was primarily to ensure representative samples in each size category, to test the hypothesis that different size categories of whale sharks (based on the median threshold) demonstrate different temporal trends in abundance.

6.3.2.4 Evidence of intrinsic and extrinsic control in SPUE rate of change

In addition to testing for a decline in the raw temporal trends in SOI-detrended SPUE, we examined the relative evidence for intrinsic (including both births and temporary immigration) and extrinsic (e.g., deterministic drivers such as over-harvest) control of the detrended relative abundance data. Our hypothesis in this case was that evidence for an exogenous (i.e., environmental or anthropogenic) driver of the decline, as revealed by the SPUE data, would be supported if density-independent models of the relationship between population rate of change (r) and relative abundance (SPUE) had stronger information-theoretic evidence than density-dependent models (an approach used for many other taxa to determine the relative contribution of extrinsic versus intrinsic control of population size - de Little et al. 2007, Chamailé-

Jammes et al. 2008, Yang et al. 2008). This hypothesis is based on the assumption that deterministic declines caused by harvest do not fluctuate with respect to stock density; this a fundamental tenet of fisheries management based on catch-per-unit-effort (CPUE) data (Walters 1995, Walters & Martell 2004, but see also Maunder et al. 2006 for the limitations of CPUE data interpretation).

We adopted a multiple-working hypotheses approach based on information-theoretic multi-model inference (Burnham & Anderson 2002) by applying two variants of the generalised θ -logistic population growth model (Turchin 2003) to the detrended SPUE series (averaged by year): (1) Gompertz-logistic growth –

$$\log\left(\frac{\text{SPUE}_{t+1}}{\text{SPUE}_t}\right) = r = r_m \left[1 - \left(\frac{\log(\text{SPUE}_t)}{\log(K)} \right)^\theta \right] + \varepsilon_t$$

where SPUE_t = SOI-detrended relative abundance time t , r = realised population growth rate, r_m = maximal intrinsic population growth rate, K = carrying capacity, θ is a shape parameter set to 1, and ε has a mean of zero and a variance (σ^2) that reflects environmental variability in r ; and (2) exponential growth (where $\theta = -\infty$, and r_m and σ are estimated).

We used MLE to fit model parameters via linear regression, and models were contrasted using AIC_c as described above. All detrended SPUE were first standardised according to the expression $y' = y + 1.1 \max(\text{abs}(y))$ to remove negative values that can be problematic for ML estimation.

6.3.3 Results

A total of 4436 sightings provided 2411 unique (per day) sightings of whale sharks from 1995 to 2004, of which 1333 records had estimates of TL and sex. The overall length-frequency distribution showed was moderately right-skewed (Fig. 6.8A) as is expected for a largely juvenile aggregation (Meekan et al. 2006, Bradshaw et al. 2007). Comparing the length-frequency distribution from 1995-1996 (Fig. 6.8B) to that from 2003-2004 (Fig. 6.8C) shows a marked shift of the frequency distribution to one dominated by smaller (< 6 m TL) individuals with few large representatives (Fig. 6.8C).

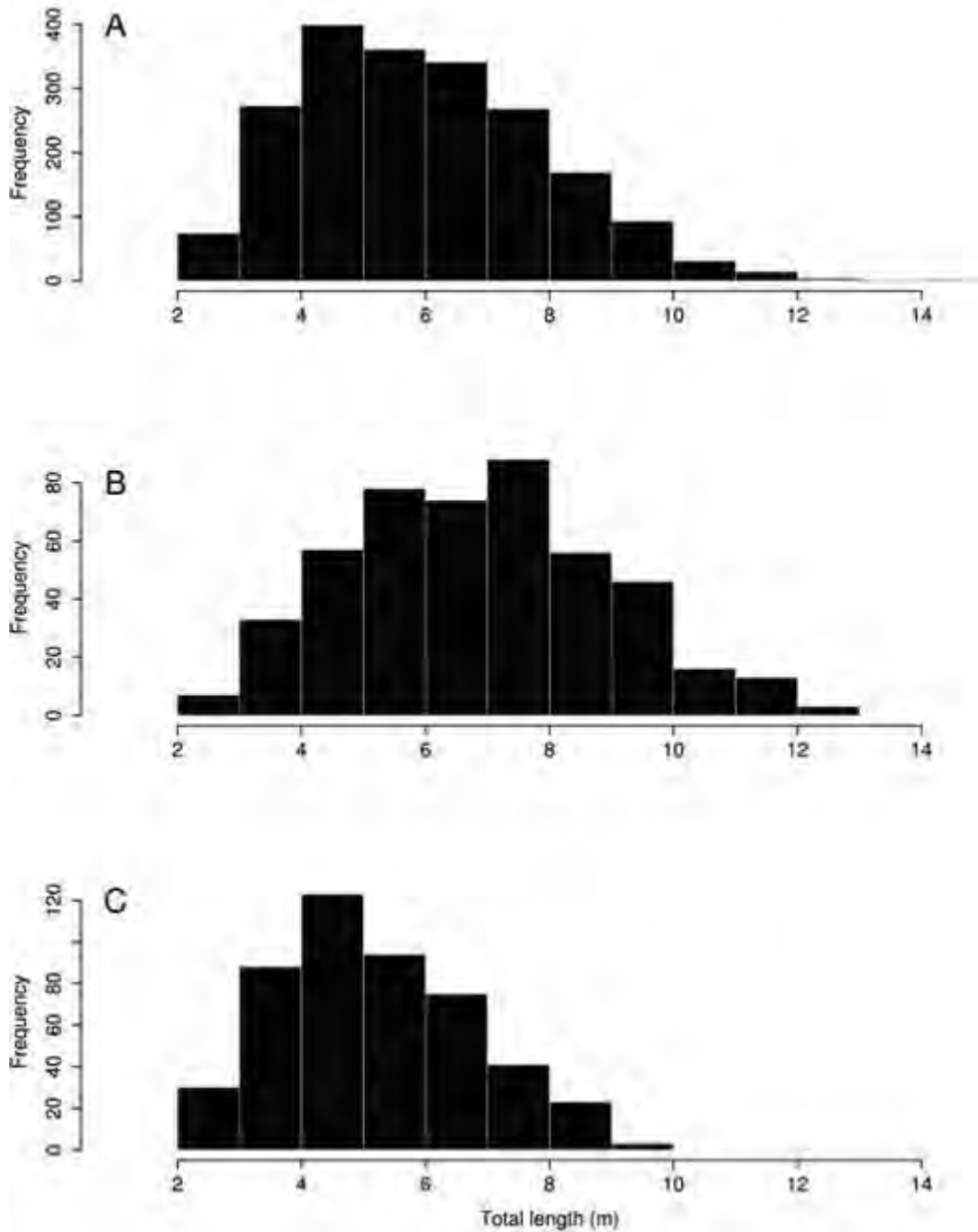


Figure 6.8. Estimated total length (TL in m) distribution for whale sharks seen at Ningaloo from A. 1995-2004, B. only 1995-1996 and C. only 2003-2004. There is a noticeable loss of larger individuals in the more recent distribution.

This can also be shown as a temporal trend; the annual mean estimates of TL showed a strong linear decline with year, explaining over 91 % of the deviance (%DE) (Table 6.4; Fig. 6.9). In 1995, whale sharks averaged 7.0 m TL (95 % 10000 iterations bootstrapped confidence interval: 6.5 – 7.4 m), but by 2004, sharks averaged only 5.4 m (5.2 – 5.6 m; Fig. 6.9). There was moderate support for the logistic model (Akaike's Information Criterion weigh [$wAIC_c$] = 0.20); however, the increase in %DE using the logistic against the linear was minor (< 3 %; Table 6.4). This implies that the decline is being driven by the faster disappearance of the remaining largest individuals – a result consistent with hypothesis that an anthropogenic source of mortality is driving the decline.

Table 6.4. Four models applied to the relationship between mean total length (TL) and year for whale sharks from Ningaloo Reef between 1995 and 2004. Models are ranked according to Akaike's Information Criterion corrected for small sample size (AIC_c). Shown for each model are the number of parameters (k), the maximum log-likelihood (LL), the difference in AIC_c for each model from the top-ranked model (ΔAIC_c), AIC_c weight ($wAIC_c$), and the percent deviance explained (%DE) in the response variable (TL).

Model	k	LL	ΔAIC_c	$wAIC_c$	%DE
linear	3	3.49	0.00	0.71	91.49
logistic	3	2.20	2.57	0.20	89.00
quadratic	4	4.53	3.93	0.09	93.08
intercept	1	-8.83	20.35	< 0.01	0.00

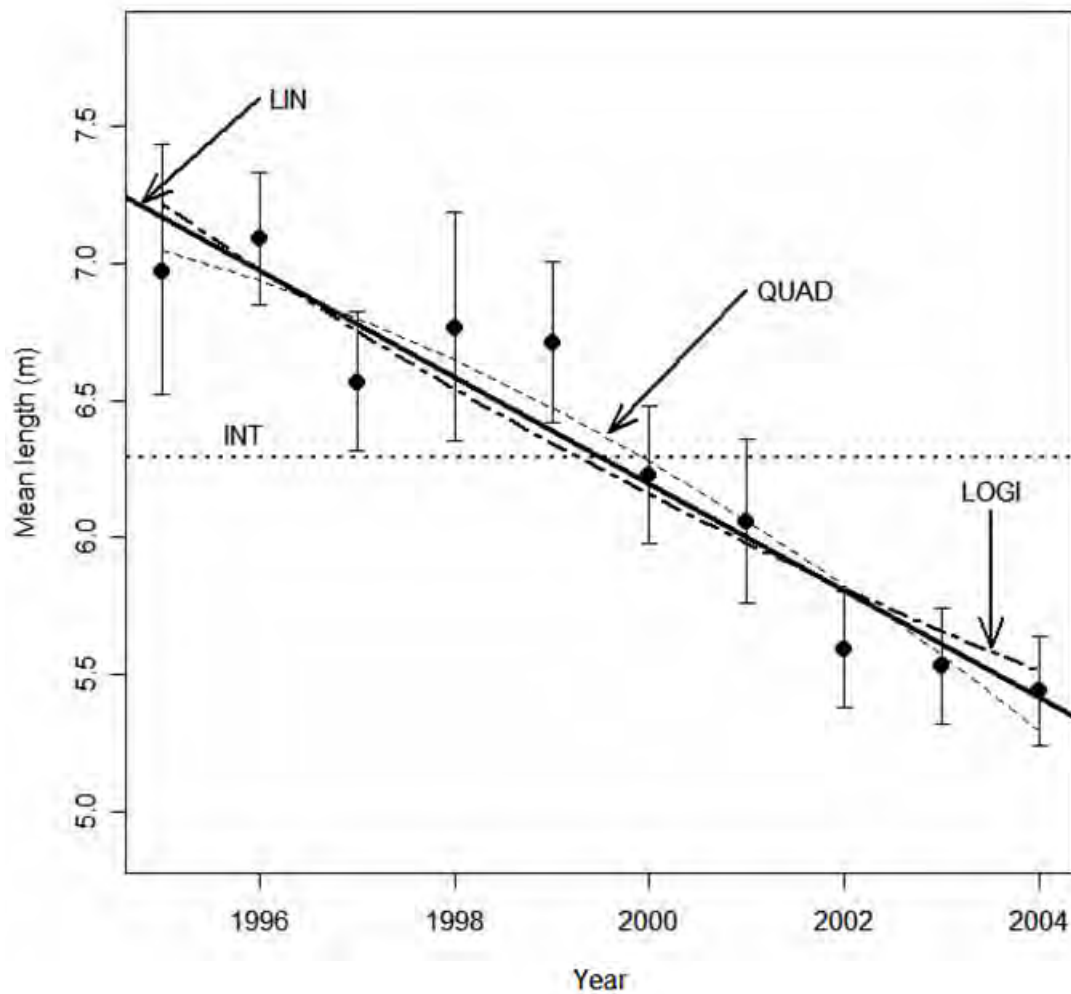


Figure 6.9. Mean length ($\pm 95\%$ bootstrapped confidence intervals based on 10 000 iterations to account for non-normal data in some years) of all whale sharks observed at Ningaloo Reef from 1995 – 2004. Information-theoretic model rankings indicated highest support for a linear decline (LIN) against the quadratic (QUAD) and logistic (LOGI) models. Relative to any of these models of decline, the intercept model (INT), characterising a stable population, had no support.

Using all data (i.e., not just annual means), we found strong support for a nested *year/month* effect on TL, but nearly no support for a *month* effect alone on %DE (Table 6.5). Including the sex term in the reduced dataset improved model fit slightly (Table 6.5), but the relatively small improvement in the % deviance explained (1.8 %) suggested that its effect was negligible (i.e., no major size differences between males and females).

Table 6.5. Comparison of general linear models (GLM) examining the relationship between total length (TL) and temporal variables for whale sharks at Ningaloo Reef from 1995 – 2004. A. TL versus *year* and *month*, and B. Five top-ranked GLMs examining the relationship between *year*, *month* and *sex* and TL. Models are ranked according to the Bayesian Information Criterion (BIC). Shown for each model are the number of parameters (*k*), the maximum log-likelihood (*LL*), the difference in BIC for each model from the top-ranked model (Δ BIC), BIC weight (*w*BIC), and the percent deviance explained (%DE) in the response variable (TL).

Model	<i>k</i>	<i>LL</i>	Δ BIC	<i>w</i> BIC	%DE
<u>A. Year & month only</u>					
TL ~ <i>year/month</i>	4	-3646.06	0.00	0.72	9.99
TL ~ <i>year</i>	3	-3650.87	2.12	0.25	9.51
TL ~ 1	2	-3741.51	175.90	< 0.01	0.00
TL ~ <i>month</i>	3	-3741.47	183.32	< 0.01	< 0.01
<u>B. Year, month & sex</u>					
TL ~ <i>sex + year</i>	4	-2676.01	0.00	0.51	11.33
TL ~ <i>sex + year/month</i>	5	-2672.44	0.07	0.49	11.80
TL ~ <i>sex + year/month + year/month*sex</i>	7	-2671.63	12.84	< 0.01	11.91
TL ~ <i>year</i>	3	-2686.35	13.49	< 0.01	9.94
TL ~ <i>sex</i>	3	-2749.52	139.83	< 0.01	0.99

Replacing the *month* factor for the *day of year* covariate changed the model rankings only marginally and overall %DE was similar (Table 6.6). The linear mixed-effects models (GLMMs) used to account for potential trends within vessels demonstrated that the model TL ~ *year/month* remained the most highly ranked ($wBIC = 0.58$), indicating a decline in TL even after accounting for any observer bias (i.e., bias accounted for by partitioning the variance among vessels in the random effect).

Table 6.6. Comparison of general linear models (GLM) examining the relationship between total length (TL) and temporal variables for whale sharks at Ningaloo Reef from 1995 – 2004. **A.** TL versus *year* and *day of year (doy)*, and **B.** Five top-ranked GLMs examining the relationship between *year*, *doy* and *sex* and TL. Models are ranked according to the Bayesian Information Criterion (BIC). Shown for each model are the number of parameters (k), the maximum log-likelihood (LL), the difference in BIC for each model from the top-ranked model (ΔBIC), BIC weight ($wBIC$), and the percent deviance explained (%DE) in the response variable (TL).

Model	k	LL	ΔBIC	$wBIC$	%DE
<u>A. Year & day-of-year only</u>					
TL ~ <i>year</i>	3	-3650.87	0.00	0.74	9.51
TL ~ <i>year/doy</i>	4	-3648.18	2.12	0.26	9.78
TL ~ 1	2	-3741.51	173.78	< 0.01	0.00
TL ~ <i>doy</i>	3	-3740.55	179.35	< 0.01	0.11
<u>B. Year, day-of-year & sex</u>					
TL ~ <i>sex + year</i>	4	-2676.01	0.00	0.91	11.33
TL ~ <i>sex + year/doy</i>	5	-2674.69	4.56	0.09	11.51
TL ~ <i>sex + year/doy + year/doy*sex</i>	7	-2671.90	13.37	< 0.01	11.87
TL ~ <i>year</i>	3	-2686.35	13.49	< 0.01	9.94
TL ~ <i>sex</i>	3	-2749.52	139.83	< 0.01	0.99

Total numbers of sharks observed from year to year varied by nearly an order of magnitude, with peaks in the 1996 and 2002 seasons, and lows in 1998 (Fig. 6.10A). Search effort (number of search hours by vessels) was also variable (Fig. 6.10A) and tended to increase through time. The sightings per unit effort (SPUE) appeared to decline through time, albeit with substantial annual variation (Fig. 6.10B). The relationship between SPUE and the SOI was strongly supported (AIC_c evidence ratio [ER] = 10.6; $R^2 = 0.28$; Fig. 6.10D), such that during years characterised by cooler El Niño events (low SOI; Fig. 6.10C), relatively fewer sharks were seen by tourist operators. This provides clarity on the earlier work demonstrating a possible relationship between whale shark abundance and ENSO-related climatic variation (Wilson et al. 2001b). SOI-detrended SPUE for all sharks combined demonstrated a gradual decline from 1995 to 2004 ($ER = 2.4$; $R^2 = 0.16$) – tourist operators saw approximately 40 % fewer sharks per hour of searching in 2004 than in 1995. This population-level result confirms life-history based predictions of decline at Ningaloo Reef (Bradshaw et al. 2007).

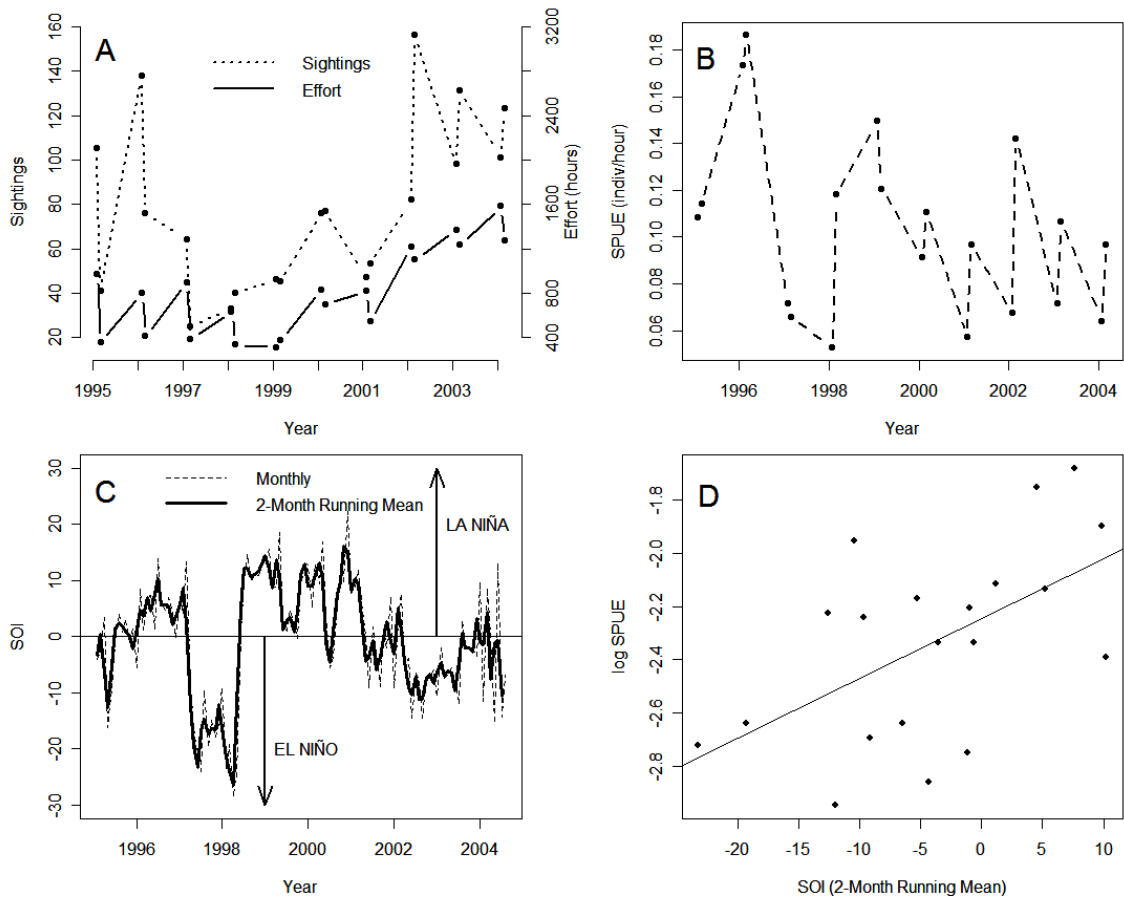


Figure 6.10. A. Total number of sharks seen at Ningaloo Reef in April and May from 1995 – 2004 after removing individuals seen more than once per day, and total vessel search time (hours) as an index of effort; B. Relative abundance corrected for effort (sightings per unit effort = SPUE); C. Monthly and two-monthly running mean of the Southern Oscillation Index (SOI) from 1995 – 2004. High positive values are indicative of La Niña conditions, whereas low negative values signal El Niño events; D. Linear relationship between the two-monthly running mean of SOI and log SPUE for all individuals combined (information-theoretic evidence ratio [ER] = 10.6 times more support than the no-change model; $R^2 = 0.28$).

There was no discernable reduction in SOI-detrended SPUE for small individuals (small males: $ER = 0.4$; $R^2 < 0.01$; small females: $ER = 0.3$; $R^2 < 0.01$; Fig. 6.11A, C), but both large male ($ER = 6.0$; $R^2 = 0.25$; Fig. 6.11B) and large female ($ER = 39.8$; $R^2 = 0.38$; Fig. 6.11D) SPUE declined substantially over the study interval, suggesting that the overall decline is driven mainly by a loss of larger individuals rather than a change in the number of smaller individuals (cf. Figures 6.8 and 6.9).

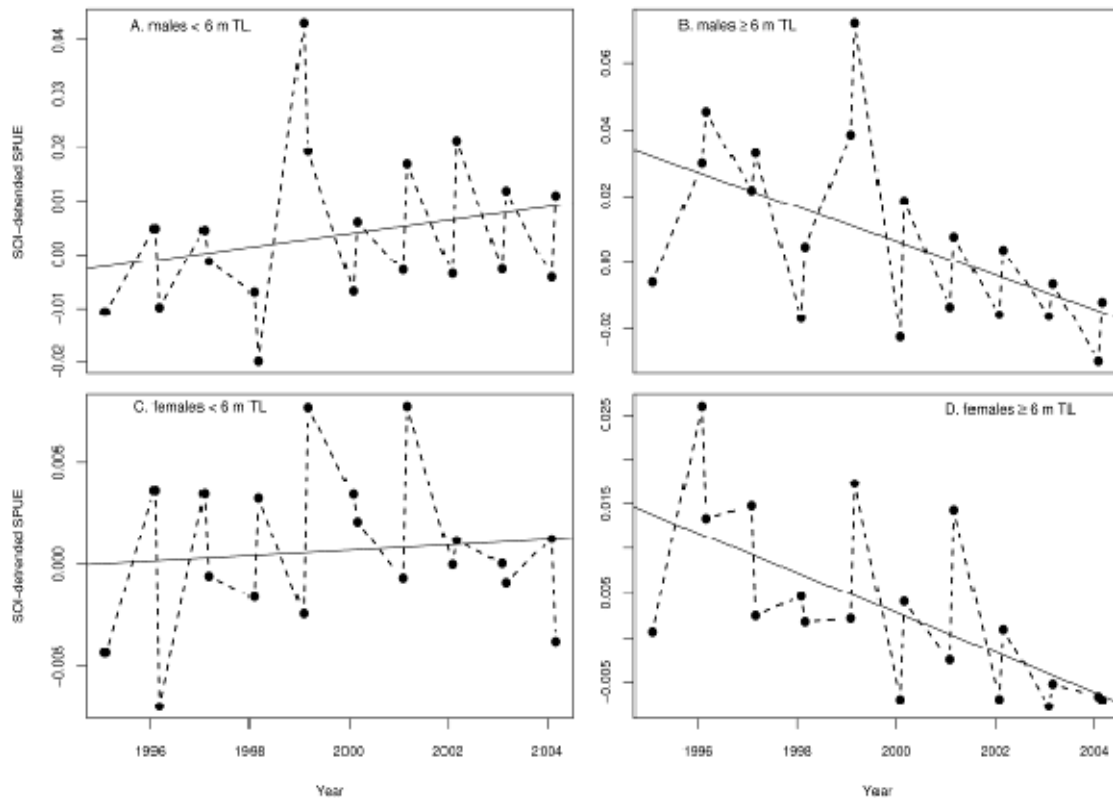


Figure 6.11. Southern Oscillation Index (SOI)-detrended whale shark sightings per unit effort (SPUE) for A. small (< 6 m total length) males (evidence ratio [ER] = 0.4; $R^2 < 0.01$), B. large (≥ 6 m TL) males ($ER = 6.0$; $R^2 = 0.25$), C. small females ($ER = 0.3$; $R^2 < 0.01$) and D. large females ($ER = 39.8$; $R^2 = 0.38$).

The relative contribution of intrinsic versus extrinsic control in the various age-sex classes provides insight into the possible mechanisms driving the observed decline. For all individuals combined ($\bar{r} = -0.015$, $\hat{\sigma}^2 = 0.24$), the Gompertz-logistic (GL) versus exponential (EX) model ranking was equivocal (little support for the GL versus EX models: $ER = 1.2$; Table 6.7; and mean r and estimated variance were $\bar{r} = -0.08$, $\hat{\sigma}^2 = 0.27$, respectively); however, there was moderate support for a density-dependent GL relationship ($ER = 2.7$; Table 6.7) for large males (Fig. 6.12), suggesting a possible negative feedback control. Large female SPUE had higher relative support for the EX model ($ER = 2.8$; Table 6.7), reinforcing the hypothesis of a deterministic reduction ($\bar{r} = -0.03$, $\hat{\sigma}^2 = 0.16$) in the large breeding females.

Table 6.7. Comparison of two population dynamical models (Gompertz-logistic and exponential) describing the relationship between rate of change in Southern Oscillation Index (SOI)-detrended whale shark sightings per unit effort (SPUE) for **A.** All individuals combined, **B.** large (≥ 6 m total length) males only and **C.** large females only. Models are ranked according to Akaike's Information Criterion corrected for small sample size (AIC_c). Shown for each model are the number of parameters (k), the maximum log-likelihood (LL), the difference in AIC_c for each model from the top-ranked model (ΔAIC_c), and AIC_c weight ($wAIC_c$).

Model	k	LL	ΔAIC_c	$wAIC_c$
<u>A. All individuals</u>				
Gompertz	3	-3.75	0.00	0.54
exponential	2	-6.31	0.31	0.46
<u>B. Large males only</u>				
Gompertz	3	-2.43	0.00	0.73
exponential	2	-5.81	1.97	0.27
<u>C. Large females only</u>				
exponential	2	-3.88	0.00	0.74
Gompertz	3	-2.51	2.06	0.26

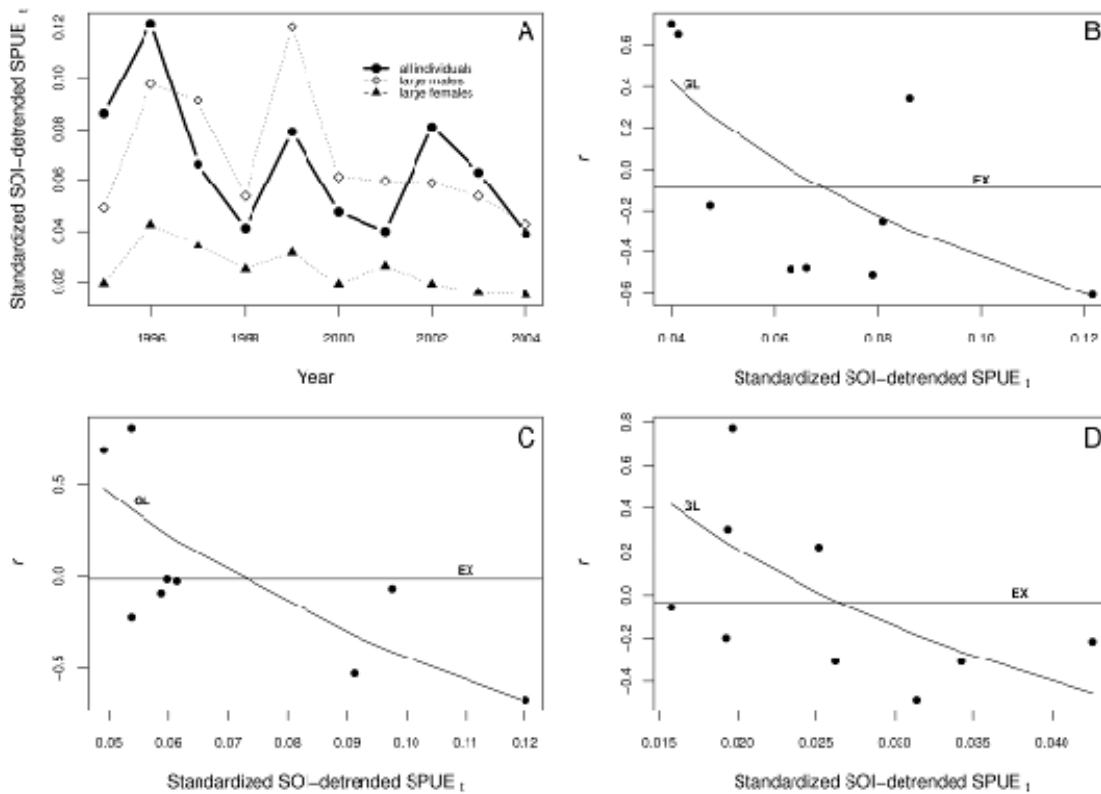


Figure 6.12. A. SOI-detrended SPUE versus year for all individuals combined, large (≥ 6 m total length) males only, and large females only; B. SOI-detrended SPUE rate of change and standardised SPUE according to the Gompertz-logistic (GL) and exponential (EX) dynamical models; C. The same relationship for large males only; D. The same relationship for large females only. Model results are presented in Table 6.6.

6.3.4 Discussion

Our results are derived from one of the largest-ever databases compiled for whale sharks. They provide empirical confirmation at the population level of the vital rate predictions of Bradshaw et al. (2007), who argued that apparent survival probability combined with plausible reproductive rates predict a declining population. While it is possible that the observed trends in mean size and relative abundance could be driven by permanent emigration of larger animals away from Ningaloo rather than an increased mortality rate, photo-identification data suggest that the Ningaloo aggregation is comprised of mainly non-transient individuals (Bradshaw et al. 2007). In other words, individuals residing at Ningaloo for a few weeks or months per year return regularly over time, at least at the decadal scale. This supports the conclusion that current survival rates are insufficient to maintain population stability or increase (Meekan et al. 2006).

The pronounced linear reduction in mean size we report here provides a robust empirical confirmation of previous results (based on a much reduced sample) that larger individuals are being lost from the Ningaloo Reef aggregation (Meekan et al. 2006). The rapid reduction in mean size we observed over a decade and the greater support for a linear model without tapering support the hypothesis of a rapid, deterministic mortality source such as harvesting. The latter evidence for exponential decline does also rely to some extent on the degree of measurement error associated with the SPUE time series. However, high measurement (observation) error tends to overinflate the evidence for density-feedback models (Brook & Bradshaw 2006), so the support of the exponential model suggests any possible bias was low. Another potential source of error is that trending populations can mask some of the evidence for endogenous mechanisms (Strong 1986), especially if the time series does not represent a large variation in densities (Speed et al. 2008). However, none of the SPUE declines measured were precipitous (\bar{r} varied from -0.015 to -0.03 for large males and females, respectively), so we expect little undue bias. Although alternative hypotheses such as an increase in ship-strike (Bradshaw et al. 2007) or entanglement rates, genetic changes and re-equilibration of population density to shifting climate patterns, cannot be rejected given the relatively short time series available, the long generation time of whale sharks (> 14 years; Speed et al. 2008) suggests that genetic and abiotic factors would likely drive much more gradual body size trends than the one we observed over a single decade. Furthermore, recent evidence that the incidence of scarring in whale sharks does not correlate well with relative mortality rates (Davis et al. 1997) suggests that non-targeted sources of anthropogenic mortality are unlikely to account for the large changes observed.

In Australia, whale sharks are protected by government legislation and are not fished or caught incidentally (Eckert et al. 2002, Wilson et al. 2006, Bradshaw et al. 2007, Castro et al. 2007). However, satellite tracking and genetic data have shown that this species has a propensity to migrate large distances (i.e., in the order of 1000s of kilometres; IUCN-SSC Shark Specialist Group 2002), implying that the geographical range of Ningaloo whale sharks is large and potentially encompasses much of Southeast Asia and the Indian Ocean. These lines of evidence – decline in relative abundance driven mainly by the disappearance of large individuals in less than a single whale shark generation, lack of evidence for a re-equilibration in mean body size, and long-distance migratory capacity – all lend support to the view that unsustainable mortality sources are occurring outside of Australia's jurisdiction. The most likely candidate is the whale shark fishery of Southeast Asia (Chen & Phipps 2002). The commercial harvest of whale sharks principally supplies markets in Taiwan, where fins (preferably from large individuals) are used for soup and the flesh is sold for human consumption (Chen et al. 1997a, Pravin 2000). Demand has driven increased fishing effort at aggregation sites throughout the Indian Ocean and Asia (Fowler 2000), although Taiwan recently announced its decision to halt commercial harvest of the species. Although many countries now have prohibited or reduced commercial harvest in recent years, there is little enforcement of regulation and it seems likely that considerable illegal and legal exploitation of whale sharks still continues throughout much of Asia (Ricker 1981, Pauly et al. 1998, Stokes & Law 2000, Tenhumberg et al. 2004).

6.3.5 Conclusions and conservation remarks

Our hypothesis that the trend observed is driven largely by over-harvesting throughout the species' range within Southeast Asia and the Indian Ocean is also consistent with declines in abundance and change in the size composition of other exploited animal populations worldwide (Gerrodette 1987). The support for the alternative hypothesis, that the decline results from an ocean-wide regime shift or climate change, is comparatively weak. Indeed, the long time series (relative to generation length) normally required to detect subtle changes in population trends (Bradshaw et al. 2007) leads us to conclude that the mechanisms driving the observed decline in whale sharks are particularly pronounced. The recent cessation of one of the last remaining commercial harvests of whale sharks in Taiwan will most likely increase the average survival probability of whale sharks in the region; however, it is unlikely that the benefits of this shift in policy will be manifested in whale shark abundance patterns for some time given the relatively slow vital rates of this large species (Bradshaw et al. 2007) and unquantified illegal and artisanal harvests elsewhere. We predict, therefore, that the downward trend in relative abundance and mean body size will continue for the foreseeable future.

Given the higher statistical likelihood that exploitation, rather than natural climate cycles, is the principal driver of the decline in abundance and body size of the world's largest fish, the precautionary principle argues for the adoption of more proactive and internationally directed conservation efforts. Although whale sharks are entirely protected in Australian waters, the seasonal outward migration of the Ningaloo population outside of Australian jurisdiction demonstrates that the observed population trend cannot be reversed by protection in only isolated parts of the species' range. Conservation of whale sharks will require international collaboration to reduce overall fishing mortality, potentially at the scale of entire ocean basins, and more tagging studies to identify migration pathways will be a vital part of this effort. Continued monitoring of relative abundance patterns, body size distributions and demographic parameters via capture-mark-recapture studies at all major aggregation sites are also important components of an ocean-wide approach to manage this species.